

ON THE SHAPE OF AVALANCHES

WEN SHEN

ABSTRACT. In this paper we study a dimensionless model of granular matter. The model can be rewritten into a system of balance laws. We prove that, every sufficiently small, compactly supported perturbation of a Lipschitz continuous decoupled initial data gives decoupled solution in finite time. Moreover, no gradient catastrophe occurs, i.e., the solution does not develop discontinuities.

Keywords: Granular matter, conservation laws, decoupled solutions, global solutions.

1. INTRODUCTION

In recent years, many research papers are devoted to the systematic study of the dynamical behavior of granular matter [3]. In this paper, we consider a model proposed in [6]. We denote by h the width of the moving layer, and by u the height of the standing layer of granular matter. The evolution of the two quantities is described by the system

$$\begin{cases} h_t &= (hu_x)_x - (1 - |u_x|)h, \\ u_t &= (1 - |u_x|)h. \end{cases} \quad (1)$$

This is a “dimensionless” model. It describes the following physical phenomenon. The moving layer slides downhill if the slope of the standing layer is larger than 1 in absolute value. The speed of the rolling layer equals to the slope of the standing layer minus 1. Clearly, the slope $|u_x| = 1$ is a critical slope, with the following property. If $|u_x| > 1$ then grains initially at rest start moving if they are hit by rolling grains of the moving layer. Hence erosion appears and the moving layer gets bigger. On the other hand, if $|u_x| < 1$, grains which are rolling can be deposited on the bed. Hence the moving layer gets smaller. Though it is a very simple model, it captures the important features in a phenomenon such as an avalanche. For more details on derivation of the model and its stationary solutions, we refer to [6].

Throughout the following, we assume $u_x \geq 0$ and drop absolute values. Differentiating the second equation in (1) and setting $p = u_x$ we obtain the system of balance laws

$$\begin{cases} h_t - (hp)_x &= (p - 1)h, \\ p_t + ((p - 1)h)_x &= 0. \end{cases} \quad (2)$$

The most interesting thing to look at in this problem is when $\bar{p} = 1$ and $\bar{h} = 0$, i.e., the slope is at the critical point, and an avalanche is about to begin. We therefore focus our attention in a small neighborhood around $(\bar{p}, \bar{h}) = (1, 0)$.

The Jacobian matrix of this system is

$$A(h, p) = \begin{pmatrix} -p & -h \\ p-1 & h \end{pmatrix},$$

and the characteristic polynomial is

$$P(\lambda) = \lambda^2 - (h-p)\lambda - h.$$

If $(p-h)^2 + 4h > 0$, this polynomial has two real distinct roots, namely

$$\lambda = \frac{h-p \pm \sqrt{(p-h)^2 + 4h}}{2}.$$

Assume now $p \approx 1$ and $h \approx 0$. Then, the leading term in the eigenvalues are

$$\lambda_1(p, h) = -p, \quad \lambda_2(h, p) = h.$$

The corresponding eigenvectors have the following leading terms

$$r_1(h, p) = \begin{pmatrix} 1 \\ \frac{p-1}{\lambda_1-h} \end{pmatrix} = \begin{pmatrix} 1 \\ \frac{1-p}{p+h} \end{pmatrix} \quad r_2(h, p) = \begin{pmatrix} \frac{-h}{p+\lambda_2} \\ 1 \end{pmatrix} = \begin{pmatrix} \frac{-h}{p+h} \\ 1 \end{pmatrix}.$$

Notice that, for all h, p ,

$$\begin{aligned} \lambda_1(h, 1) &= -1, & r_1(h, 1) &= \begin{pmatrix} 1 \\ 0 \end{pmatrix}, \\ \lambda_2(0, p) &= 0, & r_2(0, p) &= \begin{pmatrix} 0 \\ 1 \end{pmatrix}. \end{aligned}$$

Computing directional derivatives, we find

$$r_1 \bullet \lambda_1 = \frac{p-1}{p+h}, \quad r_2 \bullet \lambda_2 = -\frac{h}{p+h}. \quad (3)$$

Hence the system is weakly linearly degenerate at the point $(h, p) = (0, 1)$. The first characteristic field is genuinely nonlinear away from the line $p = 1$ and the second field is genuinely nonlinear away from the line $h = 0$. Integral curves of the eigenvectors r_1, r_2 near the neighborhood $p = 1$ and $h = 0$ are shown in Fig. 1.

2. GLOBAL EXISTENCE OF SMALL PERTURBATIONS OF DECOUPLED SOLUTIONS

By a **decoupled initial data** we mean a set of initial conditions of the form

$$h(0, x) = \phi(x) \quad p(0, x) = 1 + \psi(x) \quad (4)$$

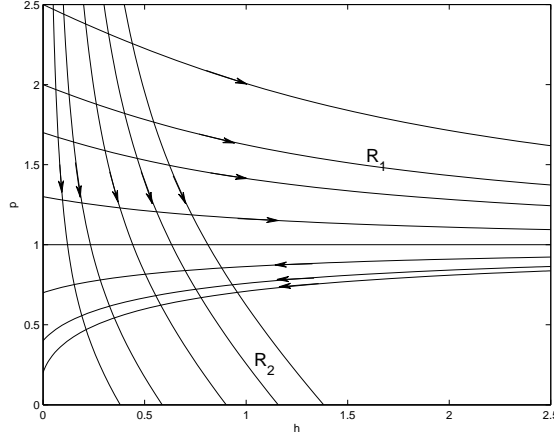


FIGURE 1. Integral curves of the two families. The arrows point in the direction of increasing eigenvalues.

with ϕ, ψ satisfying

$$\begin{cases} \phi(x) = 0 & \text{if } x \notin [a, b], \\ \psi(x) = 0 & \text{if } x \notin [c, d]. \end{cases}$$

The intervals are disjoint, i.e., $a < b < c < d$. Moreover we assume $\psi(x) > -1$ for all x .

For decoupled initial data, a global solution of the Cauchy problem can be explicitly given (see Fig. 2), namely

$$h(t, x) = \phi(x + t), \quad p(t, x) = 1 + \psi(x), \quad x \in \mathbb{R}, t \geq 0,$$

Our main goal is to prove stability of these decoupled solutions. More precisely, we show that every sufficiently small, compactly supported perturbation of a Lipschitz continuous decoupled solution eventually becomes decoupled. Moreover, no gradient catastrophe occurs.

Theorem 1. *Let $a < b < c < d$ be given, together with Lipschitz continuous, decoupled initial data as in (4). Then there exists $\delta > 0$ such that the following holds. For every perturbations $\tilde{\phi}, \tilde{\psi}$, satisfying*

$$\tilde{\phi}(x) = \tilde{\psi}(x) = 0 \quad \text{if } x \notin [a, d], \quad |\tilde{\phi}'(x)| \leq \delta, |\tilde{\psi}'(x)| \leq \delta, \quad (5)$$

the Cauchy problem for (2) with initial data

$$h(0, x) = \phi(x) + \tilde{\phi}(x), \quad p(0, x) = 1 + \psi(x) + \tilde{\psi}(x), \quad (6)$$

has a unique solution, defined for all $t \geq 0$ and globally Lipschitz continuous. Moreover, this solution becomes decoupled in finite time.

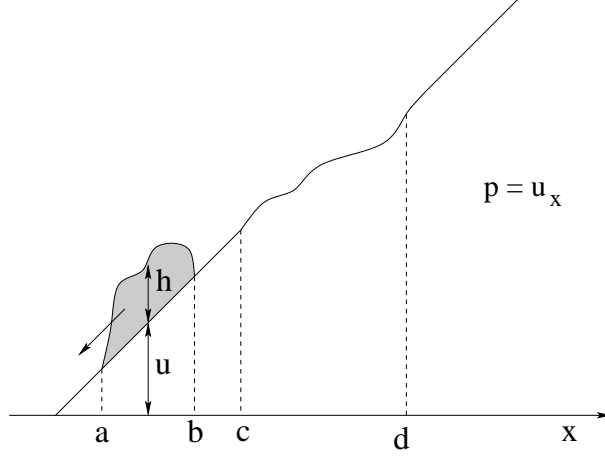


FIGURE 2. Decoupled initial data.

Proof. Since we are looking for continuous solutions, it is convenient to work in a set of Riemann coordinates. Let $(h, p) \mapsto (w, z)$ be the coordinate transformation such that

$$\begin{aligned} (w, z)(h, 1) &= (h, 0) && \text{for all } h, \\ (w, z)(0, p) &= (0, p - 1) && \text{for all } p > 0, \end{aligned}$$

and

$$r_1 \bullet z \equiv 0, \quad r_2 \bullet w = 0.$$

Notice that this last condition implies that z is constant along the integral curves of the eigenvectors r_1 , while w is constant along the integral curves of r_2 .

In these new variables, the system (2) takes the form

$$\begin{cases} w_t + \lambda_1(w, z) w_x = f(w, z), \\ z_t + \lambda_2(w, z) z_x = g(w, z). \end{cases}$$

By (2) and (3) we have

$$\begin{aligned} f(w, 0) = f(0, z) &= 0, && g(w, 0) = g(0, z) = 0, \\ \frac{\partial \lambda_1}{\partial w}(w, 0) &= 0, && \frac{\partial \lambda_2}{\partial z}(0, z) = 0. \end{aligned}$$

Therefore, for small w, z ,

$$f(w, z) = \mathcal{O}(1) \cdot wz, \quad g(w, z) = \mathcal{O}(1) \cdot wz, \quad (7)$$

$$f_w(w, z) = \mathcal{O}(1) \cdot z, \quad g_w(w, z) = \mathcal{O}(1) \cdot z, \quad (8)$$

$$f_z(w, z) = \mathcal{O}(1) \cdot w, \quad g_z(w, z) = \mathcal{O}(1) \cdot w, \quad (9)$$

$$\lambda_{1,w}(w, z) = \mathcal{O}(1) \cdot z, \quad \lambda_{2,z}(w, z) = \mathcal{O}(1) \cdot w. \quad (10)$$

Remark. Since the second equation in (2) has no forcing term, one can improve the above estimates for g , namely

$$g(w, z) = \mathcal{O}(1) \cdot wz^2, \quad g_w(w, z) = \mathcal{O}(1) \cdot z^2, \quad g_z(w, z) = \mathcal{O}(1) \cdot wz.$$

In the following, however, we shall not need these sharper bounds.

In order to bound the gradient of the perturbed solution, showing that no shock can form, we need to study the evolution equation for w_x, z_x , namely

$$\begin{cases} (w_x)_t + (\lambda_1 w_x)_x = f_w w_x + f_z z_x, \\ (z_x)_t + (\lambda_2 z_x)_x = g_w w_x + g_z z_x. \end{cases} \quad (11)$$

Since w, z vanish outside a bounded interval, we have the obvious bounds

$$|w(x)| \leq \int_x^\infty |w_x(y)| dy, \quad |z(x)| \leq \int_{-\infty}^x |z_x(y)| dy. \quad (12)$$

To establish the needed a-priori estimates, we introduce the *total strength of waves* at time t

$$V(t) \doteq \int_{-\infty}^\infty |w_x(t, x)| dx + \int_{-\infty}^\infty |z_x(t, x)| dx$$

and the *wave interaction potential*

$$Q(t) \doteq \iint_{x>y} |w_x(t, x)| |z_x(t, y)| dx dy.$$

Using (11), then (8)-(9), and finally (12), the growth of V can be estimated as

$$\begin{aligned} \frac{d}{dt} V(t) &\leq \int (|f_w w_x| + |f_z z_x| + |g_w w_x| + |g_z z_x|) dx \\ &\leq C_0 \cdot \int (|z w_x| + |w z_x|) dx \\ &\leq C_0 \cdot 2Q(t), \end{aligned}$$

for some constant C_0 . Moreover,

$$\begin{aligned} \frac{d}{dt} Q(t) &\leq V(t) \cdot \int (|f_w w_x| + |f_z z_x| + |g_w w_x| + |g_z z_x|) dx \\ &\leq 2C_0 \cdot V(t) Q(t). \end{aligned}$$

Assuming for the time being that no shocks are formed, we have

$$Q(t) \equiv 0 \quad t \geq T_0$$

where T_0 is the time needed for the two families of characteristics starting within the interval $[a, d]$ to completely cross each other. More precisely, we can take

$$T_0 \doteq \frac{d-a}{\gamma}, \quad \gamma \doteq \left[\min_{h,p} \lambda_2(h, p) - \max_{h,p} \lambda_1(h, p) \right].$$

By assumption on the initial conditions, we have an estimate of the form

$$\begin{aligned} V(0) &\leq C_1 \int_a^d \left(|\phi'(x)| + |\psi'(x)| + |\tilde{\phi}'(x)| + |\tilde{\psi}'(x)| \right) dx \\ &\leq C_1 \int_a^d \left(|\phi'(x)| + |\psi'(x)| + 1 \right) dx \doteq C_2. \end{aligned}$$

Here we need to insert the coefficient C_1 in front of the integral, because the Riemann coordinates w, z are slightly different from the original h, p coordinates. Notice that, for any $\varepsilon > 0$, by choosing $\delta > 0$ in (5) sufficiently small we can achieve

$$\gamma > 1 - \varepsilon, \quad C_1 < 1 + \varepsilon.$$

Concerning the interaction potential, at time $t = 0$ our assumptions imply

$$\begin{aligned} Q(0) &\leq C_1 \int_a^d \left(|\phi'(x)| + |\psi'(x)| + |\tilde{\phi}'(x)| + |\tilde{\psi}'(x)| \right) dx \\ &\quad \cdot C_1 \int_a^d \left(|\tilde{\phi}'(x)| + |\tilde{\psi}'(x)| \right) dx \\ &\leq C_2 C_1 (d - a) \delta. \end{aligned}$$

For any given constants T_0, C_0, C_2 , and $\varepsilon > 0$, one can find $\delta > 0$ such that any solution to the system of O.D.E's

$$\begin{cases} \frac{d}{dt} v = 2C_0 \cdot q, \\ \frac{d}{dt} q = 2C_0 \cdot vq, \end{cases} \quad \begin{cases} 0 \leq v(0) \leq C_2 \\ 0 \leq q(0) \leq C_2 C_1 (d - a) \delta. \end{cases}$$

satisfies

$$v(t) \leq v(0) + \varepsilon, \quad q(t) \leq \varepsilon \quad \text{for all } t \in [0, T_0].$$

Since we already know that $Q(t) = 0$ for $t > T_0$, by a comparison argument we deduce

$$V(t) \leq V(0) + \varepsilon, \quad Q(t) \leq \varepsilon \quad \text{for all } t \geq 0, \quad (13)$$

provided that $\delta > 0$ is chosen small enough.

The first estimate in (13) provides an a-priori bound on the total variation of the solution, valid as long as it remains continuous.

In order to achieve a point-wise bound on the gradients w_x, z_x , two more integral estimates will be needed. Call $t \mapsto x_1(t, x^*)$ the 1-characteristic starting from x^* , so that

$$\frac{\partial}{\partial t} x_1(t, x^*) = \lambda_1 \quad x_1(0, x^*) = x^*.$$

Similarly, call $t \mapsto x_2(t, x^*)$ the 2-characteristic starting from x^* .

For any given $\varepsilon > 0$, we claim that, choosing $\delta > 0$ sufficiently small, one has the estimates

$$\int_{-\infty}^{x_1(t, x^*)} |z_x(t, x)| dx \leq \varepsilon \quad \text{for all } t \geq 0, \quad (14)$$

and

$$\int_0^\infty |z_x(t, x_1(t, x^*))| dt \leq \varepsilon, \quad (15)$$

for every 1-characteristic starting from a point $x^* < c$. Similarly, choosing $\delta > 0$ small, for every 2-characteristic starting from a point $x^* > b$ one can achieve

$$\int_{x_2(t, x^*)}^\infty |w_x(t, x)| dx \leq \varepsilon \quad \text{for all } t \geq 0, \quad (16)$$

and

$$\int_0^\infty |w_x(t, x_2(t, x^*))| dt \leq \varepsilon. \quad (17)$$

To establish (14)-(15), let $\varepsilon > 0$ and $x^* < c$ be given. Consider the functions

$$\begin{aligned} V^*(t) &\doteq \int_{-\infty}^{x_1(t, x^*)} |z_x(t, x)| dx, \\ Q^*(t) &\doteq \iint_{y < x < x_1(t, x^*)} |w_x(t, x)| |z_x(t, y)| dx dy. \end{aligned}$$

Starting from the second equation in (11), using (8)-(9) we obtain the inequalities

$$\begin{aligned} \frac{d}{dt} V^*(t) &\leq \left[\int_{-\infty}^{x_1(t, x^*)} (|g_w w_x| + |g_z z_x|) dx \right] - (\lambda_2 - \lambda_1) \cdot |z_x(t, x_1(t, x^*))| \\ &\leq C_0 \cdot \left[\int_{-\infty}^{x_1(t, x^*)} (|z w_x| + |w z_x|) dx \right] - \gamma \cdot |z_x(t, x_1(t, x^*))| \\ &\leq 2C_0 \cdot V(t)V^*(t) - \gamma \cdot |z_x(t, x_1(t, x^*))|, \end{aligned} \quad (18)$$

Notice that the negative terms take into account the outgoing flux across the 1-characteristic. We used here the obvious estimates

$$\int |w_x(t, x)| dx \leq V(t), \quad |z(t, x)| \leq V^*(t) \quad \text{for all } x \leq x_1(t, x^*).$$

Concerning the initial conditions, our assumptions imply

$$V^*(0) \leq C_1(c - a)\delta. \quad (19)$$

According to (13), the total variation remains uniformly bounded, say

$$V(t) \leq C_3 \quad t \geq 0. \quad (20)$$

We can now choose $\delta > 0$ such that the solution to the scalar Cauchy problem

$$\frac{d}{dt} v^* = 2C_0 C_3 v^*, \quad v^*(0) = C_1(c - a)\delta,$$

satisfies

$$v^*(t) \leq \varepsilon \quad t \in [0, T_0].$$

Recalling that the solution is decoupled after time T_0 a standard comparison argument yields

$$V^*(t) \leq \varepsilon \quad \text{for all } t \geq 0. \quad (21)$$

This proves (14).

Next, integrating the first and last terms in (18) one obtains

$$\gamma \int_0^{T_0} |z_x(t, x_1(t, x^*))| dt \leq V^*(0) - V^*(T_0) + 2C_0 \int_0^{T_0} V(t) V^*(t) dt.$$

Therefore, recalling (19), (20), and (21),

$$\int_0^{T_0} |z_x(t, x_1(t, x^*))| dt \leq \gamma^{-1}(\varepsilon + 2C_0 \cdot T_0 C_6 \varepsilon). \quad (22)$$

For $t > T_0$ we have $z(t, x_1(t, x^*)) = z(t, x_1(t, x^*)) = 0$, hence the estimate in (22) remains valid if we replace the upper limit of integration by $+\infty$. Since $\varepsilon > 0$ is arbitrary, this establishes (15). The proof of the estimates (16)-(17) is entirely similar.

We are now ready to prove the pointwise bounds on the gradients of the solution. By assumption, the initial data are uniformly Lipschitz continuous, so that

$$|w_x(0, x)| \leq M, \quad |z_x(0, x)| \leq M,$$

for some constant M and all $x \in \mathbb{R}$. We claim that, by possibly choosing an even smaller $\delta > 0$, the solution of (2) with initial data as in (5)-(6) satisfies

$$\|w_x(t, \cdot)\|_{\mathbf{L}^\infty} \leq 2M, \quad \|z_x(t, \cdot)\|_{\mathbf{L}^\infty} \leq 2M \quad \text{for all } t \geq 0. \quad (23)$$

Our claim will be proved by the following argument: if

$$\|w_x(t, \cdot)\|_{\mathbf{L}^\infty} \leq 3M, \quad \|z_x(t, \cdot)\|_{\mathbf{L}^\infty} \leq 3M$$

for all $t \in [0, \tau]$, then in fact (23) holds on the whole interval $[0, \tau]$. Since the maps

$$t \mapsto \|w_x(t, \cdot)\|_{\mathbf{L}^\infty}, \quad t \mapsto \|z_x(t, \cdot)\|_{\mathbf{L}^\infty},$$

are Lipschitz continuous, this implies that the bounds (23) hold for all times $t \geq 0$.

The equations (11) can be written in the more convenient form

$$\begin{cases} w_{xt} + \lambda_1 w_{xx} &= f_w w_x - \lambda_{1,w} w_x^2 + f_z z_x - \lambda_{1,z} w_x z_x, \\ z_{xt} + \lambda_2 z_{xx} &= g_w w_x - \lambda_{2,w} w_x z_x + g_z z_x - \lambda_{2,z} z_x^2. \end{cases}$$

According to (8)-(10) we have

$$\begin{cases} |w_{xt} + \lambda_1 w_{xx}| \leq C_0 \cdot \left(|z|(1 + |w_x|)|w_x| + |w|(1 + |w_x|)|z_x| \right), \\ |z_{xt} + \lambda_2 z_{xx}| \leq C_0 \cdot \left(|z|(1 + |z_x|)|w_x| + |w|(1 + |z_x|)|z_x| \right), \end{cases}$$

We shall derive an a-priori bound on w_x by estimating its growth along 1-characteristics. Notice that it is not restrictive to assume $t \leq T_0$. Indeed, for $t > T_0$ the solution decouples in two traveling waves, moving away from each other. Two separate cases will be considered.

CASE 1: The 1-characteristic starts from a point $x^* < c$. We then have

$$\frac{d}{dt} |w_x(t, x_1(t, x^*))| \leq C_0 |z|(1 + 3M) |w_x| + |w|(1 + 3M) |z_x|. \quad (24)$$

Therefore, recalling the uniform bound

$$|w(t, x)| + |z(t, x)| \leq V(t) \leq C_3$$

and using the estimates (14)-(15), we obtain

$$\begin{aligned} |w_x(t, x_1(t, x^*))| &\leq \left(|w_x(0, x^*)| + \int_0^t \left(|w|(1 + 3M)|z_x| \right)(t, x_1(t, x^*)) dt \right) \\ &\quad \cdot \exp \left\{ \int_0^t C_0(1 + 3M) |z(s, x_1(s, x^*))| ds \right\} \\ &\leq (M + C_3(1 + 3M) \varepsilon) \cdot \exp \{ T_0 C_0(1 + 3M) \varepsilon \} \\ &\leq 2M, \end{aligned}$$

provided that $\varepsilon > 0$ is sufficiently small.

CASE 2: The 1-characteristic starts from a point $x^* > b$. In this case, the initial data satisfies

$$|w_x(0, x^*)| \leq C_1 \delta.$$

From the equation (24) we now derive the estimate

$$\begin{aligned} |w_x(t, x_1(t, x^*))| &\leq \left(|w_x(0, x^*)| + \int_0^t \left(|w|(1 + 3M)|z_x| \right)(t, x_1(t, x^*)) dt \right) \\ &\quad \cdot \exp \left\{ \int_0^t C_0(1 + 3M) |z(s, x_1(s, x^*))| ds \right\} \\ &\leq \left(C_1 \delta + T_0 \varepsilon (1 + 3M) 3M \right) \cdot \exp \{ T_0 C_0(1 + 3M) C_3 \}. \quad (25) \end{aligned}$$

By choosing $\varepsilon > 0$, then $\delta > 0$ sufficiently small, the right hand side of (25) can be made arbitrarily small, in particular $\leq 2M$. This completes the proof.

3. CONCLUDING REMARKS AND FURTHER DISCUSSION

Remark 1. Although the solutions considered in this paper decouple and remain smooth globally, we do not expect this to be true for general initial data. Since the characteristic fields are not linearly degenerate, when the initial data contain a large gradient we expect that discontinuities will form in finite time.

From the general theory of balance laws, it is known that in any weak solution all shocks must satisfy the Rankine-Hugoniot equations

$$s \begin{pmatrix} H^r - H^l \\ P^r - P^l \end{pmatrix} = \begin{pmatrix} H^l P^l - H^r P^r \\ (P^r - 1)H^r - (P^l - 1)H^l \end{pmatrix}. \quad (26)$$

In addition, to achieve stability of solutions one should impose some additional entropy conditions. Since the characteristic fields are not linearly degenerate or genuinely nonlinear, in the present case the Liu entropy conditions [8], [9] are more appropriate. As shown in [2], these conditions uniquely characterize the weak solutions obtained as limits of vanishing viscosity approximations. Local existence and uniqueness of solutions with bounded variation can be obtained combining the analysis in [1] and in [5].

Remark 2. It is interesting to check if the equations have meaningful solutions also when the slope p changes sign. Since the basic model (1) does not account for the conservation of momentum, one might wonder if the predictions are realistic, also in cases where $p \approx 0$ and the actual motion of the granular matter may be dominated by inertial forces.

Allowing sign changes in p , the system of balance laws takes the form

$$\begin{cases} h_t - (hp)_x = (|p| - 1)h, \\ p_t + (|p| - 1)h_x = 0. \end{cases} \quad (27)$$

Notice that now the flux is no longer smooth but only Lipschitz continuous. The Jacobian matrix is

$$A(h, p) = \begin{pmatrix} -p & -h \\ |p| - 1 & \text{sign}(p)h \end{pmatrix},$$

where $\text{sign}(p)$ is the sign function of p . The two eigenvalues are

$$\lambda = \frac{\text{sign}(p)h - p \pm \sqrt{(\text{sign}(p)h - p)^2 + 4h}}{2}.$$

The characteristic curves are symmetric about h -axis in the h - p plane, but the ordering of the two characteristic families, according to increasing wave speed, is reversed (see Figure 3).

Two cases are of interests, describing the top of a mountain and the bottom of a valley.

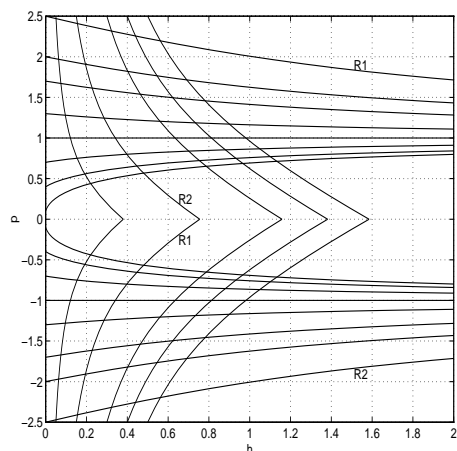
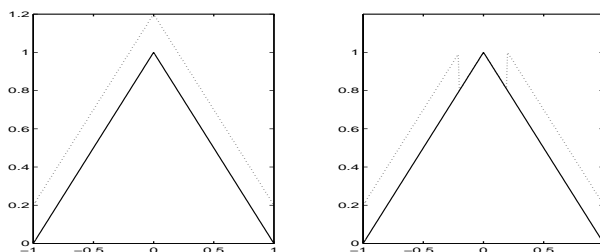


FIGURE 3. Integral curves of the two families.

The case of a sharp mountain top is very simple. We are assuming here an initial condition such that $h(0, \cdot)$ is continuous and strictly positive, while

$$\begin{cases} p(0, x) \leq -\alpha < 0 & \text{if } x < 0, \\ p(0, x) \geq \alpha & \text{if } x > 0. \end{cases}$$

In this case, the top of the mountain will always remain located at $x = 0$, while the solution simply decouples into a backward moving avalanche, on the half line $x < 0$, and a forward moving one, on the half line $x > 0$. See Figure 4 for an illustration.

FIGURE 4. The mountain top (solid lines) with moving layer (dashed line), initially (left) and at $t = 2$ (right).

A more interesting case is the smooth valley bottom. We describe here the results of some numerical simulations, taking an initial data:

$$p(0, x) = u_x(0, x) = \begin{cases} -1 & \text{for } x < -1, \\ x & \text{for } |x| < 1, \\ 1 & \text{for } x > 1. \end{cases}$$

Initially, all of the moving layer h is placed on the region where $x > 1$, and hence $p(0, x) = 1$. Our numerical scheme is a simple explicit Lax-Friedrich scheme with fine grid $\Delta x = 10^{-4}$. We tested different initial distributions for the moving layer h , all having the same total mass $m = 0.8$.

- (a). A box-shaped profile: $h = 0.2$ for $x \in [1, 1.4]$;
- (b). A hat-shaped profile on the interval $x \in [1, 1.4]$, with $h = 0.4$ at $x = 1.2$;
- (c). A box-shaped with $h = 0.02$ for $x \in [1, 4]$;
- (d). A box-shaped with $h = 0.01$ for $x \in [1, 8]$.

The simulations show that the moving layer slides down into the valley, and eventually becomes entirely deposited, partly filling the bottom of the valley. The final profiles of the valley, for different shapes of the avalanche, are plotted in Figure 5.

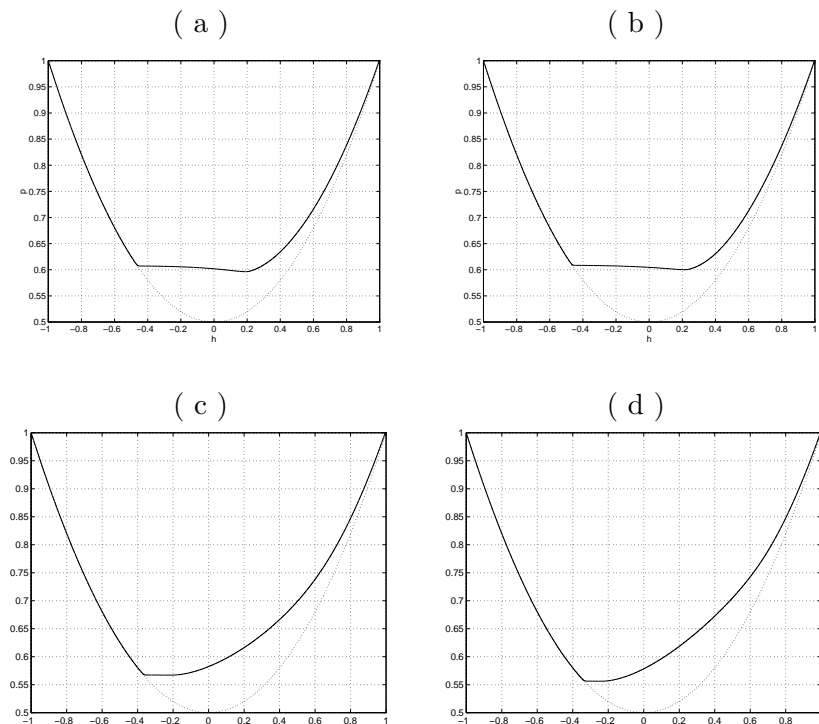


FIGURE 5. Final valley profiles on the interval $x \in [-1, 1]$, after an initial moving layer $h(0, \cdot)$ has fully deposited. The dotted lines correspond to the initial mountain shape.

We observe that:

- (i): The moving layer can reach points well to the left of the initial bottom of the valley (i.e., points where $x < 0$). This happens because the granular matter is

initially deposited on the right side (for $x > 0$). Hence the height u of the mountain becomes higher for $x > 0$, and the lowest point of the valley is moved to the left.

–(ii): In cases (a) and (b), where the initial avalanche profiles have the same support, the terminal shapes of the valley u are nearly the same.

–(iii): When the norm $\|h\|_{\mathbf{L}^\infty}$ is very small, i.e., when the deposition is very slow, the final shape of the valley depends only on the initial profile u and the total amount of mass of initial h . See (c) and (d). In fact, we tried a couple of other simulations, with different initial avalanche profiles $h(0, \cdot)$, but keeping the same total mass $\|h(0, \cdot)\|_{\mathbf{L}^1} = 0.8$ and $\|h(0, \cdot)\|_{\mathbf{L}^\infty}$ very small. In all cases, the final shape u of the valley remains almost the same as in (c) and (d).

One may conclude that this simple model captures fairly well the motion of an avalanche, also when the slope p of the mountain changes signs.

Furthermore we conjecture that, in the slow erosion (or deposition) limit as $\|h\|_\infty \rightarrow 0$, the evolution of the mountain profile is solely determined by the total amount of granular matter flowing down the slope, not by the particular shape of the avalanche. A precise result in this direction will be given in a forthcoming paper.

REFERENCES

- [1] F. Ancona and A. Marson, Well-posedness for general 2×2 systems of conservation laws. *Mem. Amer. Math. Soc.* **169** (2004), no. 801.
- [2] S. Bianchini and A. Bressan, Vanishing viscosity solutions of nonlinear hyperbolic systems. *Annals of Math.* **161** (2005), 223–342.
- [3] T. Boutreux and P. G. Gennes, Surface flows of granular mixtures, I. General principles and minimal model. *J. Phys. I France*, **6** (1996), 1295–1304.
- [4] P. Cannarsa and P. Cardaliaguet, Representation of equilibrium solutions to the table problem for growing sandpiles. *J. Eur. Math. Soc. (JEMS)*, **6** (2004), 435–464.
- [5] G. Crasta and B. Piccoli, Viscosity solutions and uniqueness for systems of inhomogeneous balance laws. *Discrete Contin. Dynam. Systems* **3** (1997), 477–502.
- [6] K. P. Haderer and C. Kuttler, Dynamical models for granular matter. *Granular Matter*, **2** (1999), 9–18.
- [7] Ta Tsien Li, *Global classical solutions for quasilinear hyperbolic systems*. John Wiley & Sons, Chichester, 1994.
- [8] T. P. Liu, The entropy condition and the admissibility of shocks. *J. Math. Anal. Appl.* **53** (1976), 78–88.
- [9] Admissible solutions of hyperbolic conservation laws. *Memoirs Am. Math. Soc.* **30**, No. 240 (1981).

DEPARTMENT OF MATHEMATICS, PENN STATE UNIVERSITY, UNIVERSITY PARK, PA 16802, U.S.A.